miR-21 mediates fibrogenic activation of pulmonary fibroblasts and lung fibrosis

Gang Liu,[1] Arnaud Friggeri,[1] Yanping Yang,[1] Jadranka Milosevic,[2] Qiang Ding,[1] Victor J. Thannickal,[1] Naftali Kaminski,[2] and Edward Abraham[1]

[1]Department of Medicine, University of Alabama at Birmingham, Birmingham, AL 35294
[2]Dorothy P. and Richard P. Simmons Center for Interstitial Lung Diseases, University of Pittsburgh School of Medicine, Pittsburgh, PA 15213

Uncontrolled extracellular matrix production by fibroblasts in response to tissue injury contributes to fibrotic diseases, such as idiopathic pulmonary fibrosis (IPF), a progressive and ultimately fatal process that currently has no cure. Although dysregulation of miRNAs is known to be involved in a variety of pathophysiologic processes, the role of miRNAs in fibrotic lung diseases is unclear. In this study, we found up-regulation of miR-21 in the lungs of mice with bleomycin-induced fibrosis and also in the lungs of patients with IPF. Increased miR-21 expression was primarily localized to myofibroblasts. Administration of miR-21 antisense probes diminished the severity of experimental lung fibrosis in mice, even when treatment was started 5–7 d after initiation of pulmonary injury. TGF-β1, a central pathological mediator of fibrotic diseases, enhanced miR-21 expression in primary pulmonary fibroblasts. Increasing miR-21 levels promoted, whereas knocking down miR-21 attenuated, the pro-fibrogenic activity of TGF-β1 in fibroblasts. A potential mechanism for the role of miR-21 in fibrosis is through regulating the expression of an inhibitory Smad, Smad7. These experiments demonstrate an important role for miR-21 in fibrotic lung diseases and also suggest a novel approach using miRNA therapeutics in treating clinically refractory fibrotic diseases, such as IPF.

CORRESPONDENCE
Gang Liu:
gliu@uab.edu

Abbreviations used: α-SMA, α-smooth muscle actin; ECM, extracellular matrix; IPF, idiopathic pulmonary fibrosis; ISH, in situ hybridization; LNA, locked nucleic acid; miRNA, microRNA.

Fibroblast proliferation and generation of provisional extracellular matrix (ECM) are primary tissue responses to injury (Tomasek et al., 2002). Successful wound repair processes are tightly regulated, with a balance of ECM synthesis and resolution as well as reepithelization (Tomasek et al., 2002). Uncontrolled ECM production can lead to clinically important fibrotic diseases, including idiopathic pulmonary fibrosis (IPF) (Tomasek et al., 2002; Thannickal et al., 2004). An important pathological feature of IPF is the presence of fibroblastic foci in the lungs, and the presence and extent of such fibroblastic foci is one of the most reliable markers of poor prognosis in patients with IPF (Wynn, 2007; Hardie et al., 2009). Fibroblastic foci are aggregations of fibroblasts/myofibroblasts that produce excessive ECM components (Wynn, 2007; Hardie et al., 2009). TGF-β1 has been shown to be an important mediator of lung fibrosis and can induce differentiation of pulmonary fibroblasts into myofibroblasts characterized by α-smooth muscle actin (α-SMA) expression and active synthesis of ECM proteins (Lee et al., 2006; Cutroneo et al., 2007).

microRNAs (miRNAs) are a class of noncoding small RNAs, 22 nt in length, which bind to the 3′ UTR of target genes and thereby repress translation of target genes and/or induce degradation of target gene mRNA (Stefani and Slack, 2008). miRNAs play essential roles in numerous cellular and developmental processes, including intracellular signaling pathways and organ morphogenesis (Stefani and Slack, 2008). Aberrant expression of miRNAs is closely associated with initiation and progression of pathophysiologic processes including diabetes, cancer, and cardiovascular disease (Thum et al., 2008; Croce, 2009; Latronico and Condorelli, 2009; Pandey et al., 2009). However, the role of miRNAs in lung fibrosis

The Rockefeller University Press $30.00
J. Exp. Med. Vol. 207 No. 8 1589-1597
www.jem.org/cgi/doi/10.1084/jem.20100035

is just beginning to unravel (Pandit et al., 2010). Therefore, determining the roles of specific miRNAs involved in the pathogenesis of lung fibrosis is likely to suggest important new directions for the treatment of IPF and other interstitial lung diseases.

In the present study, we explored the role of miRNA in the pathogenesis and progression of lung fibrosis. We found that miR-21 is highly up-regulated in the lungs of mice with bleomycin-induced lung fibrosis and in the lungs of patients with IPF. The enhanced expression of miR-21 is primarily located to myofibroblasts in the fibrotic lungs. In addition, miR-21 is up-regulated by TGF-β1 and functions in an amplifying circuit to enhance the fibrogenic activity of TGF-β1 in human primary fibroblasts. More importantly, we found that miR-21 sequestration in mouse lungs attenuates bleomycin-induced lung fibrosis. Overall, these data suggest that miR-21 is a central mediator in the pathogenesis of lung fibrosis and a potential target for developing novel therapeutics in treating fibrotic diseases, including IPF.

RESULTS AND DISCUSSION

To investigate if miRNAs may participate in the pathogenesis and progression of lung fibrosis, we identified miRNAs whose expression was altered in fibrotic lungs. A miRNA array assay was performed on RNA isolated from the lungs of mice that had been given intratracheal PBS or bleomycin for 1 or 2 wk, a well-characterized model of lung fibrosis (Moore and Hogaboam, 2008). We found that a number of miRNAs had significantly altered expression in bleomycin-exposed lungs (Fig. S1, A and B). Of these miRNAs, miR-21 demonstrated the greatest increase in expression. miR-21 has previously been shown to be induced in TGF-β1–treated human vascular smooth muscle cells and to regulate the expression of genes involved in the contraction of smooth muscle (Davis et al., 2008). Because TGF-β1 is a central pathological mediator of lung fibrosis (Cutroneo et al., 2007; Moore and Hogaboam, 2008), the induction of miR-21 by TGF-β1 suggests that miR-21 may have a potential role in the pathogenesis of lung fibrosis. To validate the miRNA array data, Northern blotting was performed and showed that miR-21 was up-regulated in lungs from bleomycin-exposed mice as early as d 3 after bleomycin administration, reached its highest levels on d 14, and remained at the highest level until at least 24 d after bleomycin administration (Fig. 1 A). Real-time PCR analysis on the same set of samples demonstrated similar results to Northern blotting (Fig. 1 B). Of note, expression of the extracellular matrix protein, fibronectin, was also up-regulated with similar timing as to miR-21 (Fig. 1 C). These data suggest that the enhanced expression of miR-21 is involved in the progression of lung fibrosis.

To demonstrate if TGF-β1 contributed to the enhanced expression of miR-21 in the fibrotic lungs, we examined pulmonary levels of TGF-β1 and found that, similar to miR-21, TGF-β1 expression started to rise at d 3 after bleomycin administration and reached maximal levels on d 7 (Fig. 1 D). TGF-β1 returned to basal levels on d 24 after bleomycin administration, consistent with previous studies (Zhang et al., 1995). To further delineate the role of TGF-β1 in the enhanced expression of miR-21 in fibrotic lungs, we used transgenic mice that inducibly express a dominant-negative form of TGF-β1RII (Ambalavanan et al., 2008), which can inhibit TGF-β1 downstream signaling events by blocking TGF-β1–induced formation of endogenous TGF-β1RI-II complex. As shown in Fig. S1 C, the enhanced expression of miR-21 was significantly attenuated in the mice expressing dominant-negative TGF-β1RII after bleomycin administration. These results suggest that TGF-β1 plays an important role in mediating the increased expression of miR-21, although other mechanisms may also be involved.

In situ hybridization (ISH) of mouse lungs showed only minimal cytoplasmic staining for miR-21, but dramatic increases after bleomycin treatment (Fig. 1 E, i-ii). The expression of miR-21 appeared in sheets in the lung parenchyma, consistent with the pattern of fibroblast/myofibroblast accumulation in bleomycin-treated lungs (Fig. 1 E, ii). In contrast, there was only minimal background staining using control probes with scrambled sequence, supporting the specificity of the miR-21 staining (Fig. 1 E, iii). To determine if miR-21 was indeed expressed in pulmonary myofibroblasts in bleomycin-treated lungs, immunohistochemistry was performed along with ISH and demonstrated that miR-21 expression was primarily colocalized with that for α-SMA (Fig. 1 F), suggesting that myofibroblasts were the main source of the increased miR-21 levels present in bleomycin-treated lungs. Lungs from patients with IPF also showed increased expression of miR-21 (Fig. 1 G), with expression primarily localized to the fibroblastic foci (Fig. 1 H, i). Taken together, these data suggest that miR-21 may participate in the pathogenesis of lung fibrosis by regulating fibroblast/myofibroblast activation.

To determine if miR-21 is involved in the development of experimental lung fibrosis, we used locked nucleic acid (LNA)–modified miR-21 antisense probes to modulate miR-21 expression. LNA-modified miRNA antisense probes were previously shown to be capable of effectively sequestering miR-122 in vivo by forming duplexes with this miRNA (Elmén et al., 2008). Intratracheal instillation of miR-21 antisense probes before bleomycin administration completely sequestered miR-21, as demonstrated by the formation of miR-21:anti-miR-21 duplexes (bands with retarded migration) in lungs harvested 2 wk after bleomycin administration (Fig. 2 A). Real-time PCR demonstrated no mature miR-21 expression in miR-21 antisense probe-treated lungs, whereas the expression of an unrelated miRNA, miR-155, was not affected by administration of the miR-21 antisense probes, consistent with specific targeting of miR-21 by the antisense probes (Fig. 2 B). Treatment with miR-21 antisense probes prevented the enhanced collagen deposition (Fig. 2 C) and elevated expression of ECM proteins, such as Fn and collagen, at both RNA and protein levels that occur in the lungs after bleomycin

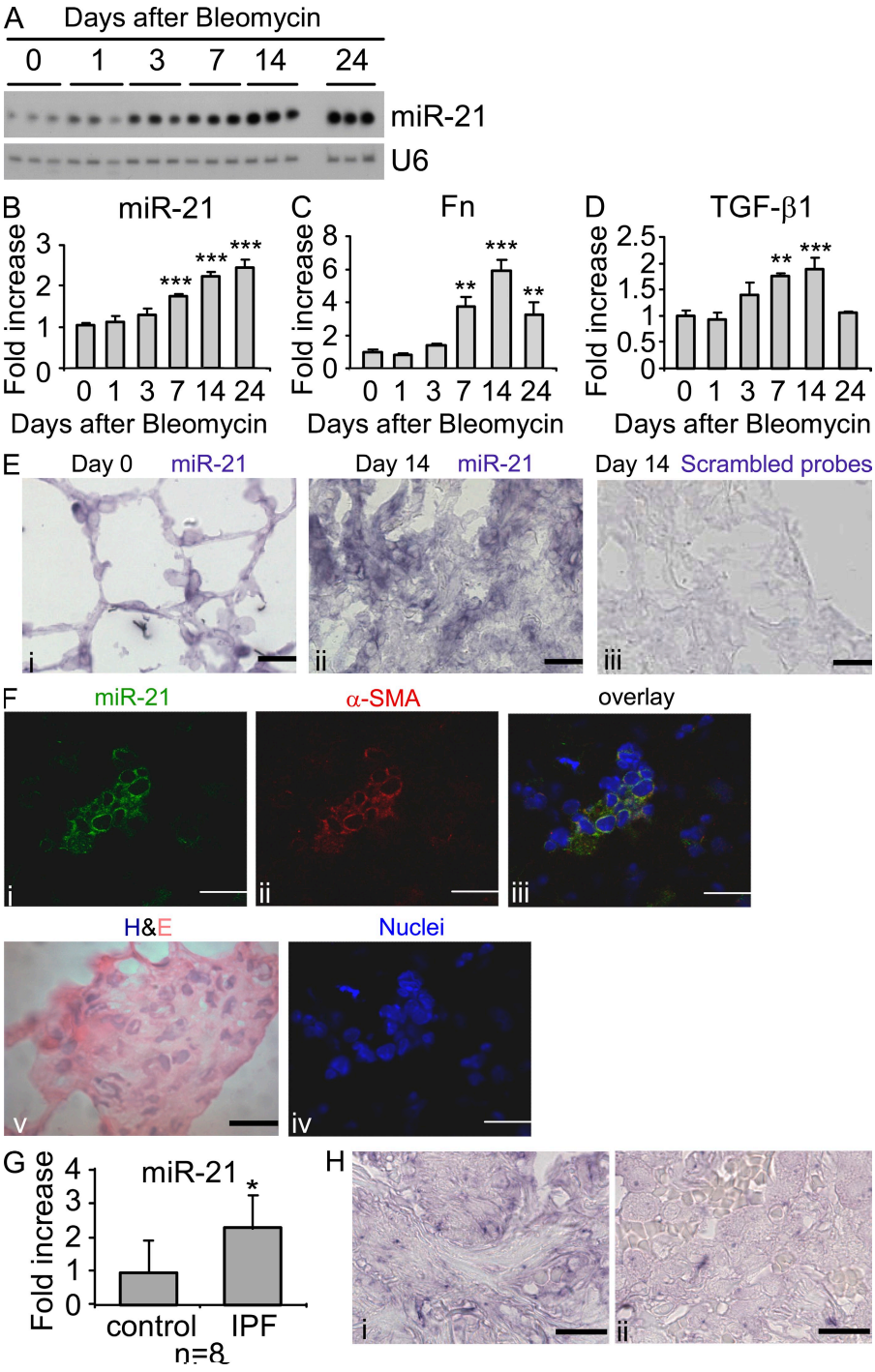

Figure 1. miR-21 is up-regulated in lungs from bleomycin-treated mice and from patients with IPF. (A) Total RNA was isolated from lungs harvested at the indicated time points after intratracheal bleomycin instillation (1.5 U/kg in 50 µl PBS). Northern blotting was performed to determine the levels of miR-21 and the loading control, small nucleolar RNA U6. (B-D) Real-time PCR was performed to determine the levels of miR-21 (B), fibronectin (C), and TGF-β1 (D) in the same samples as in A. $n = 3$ mice in each group, mean ± SEM. **, $P < 0.01$; ***, $P < 0.001$ compared with d 0. (E) Frozen sections were prepared from mouse lungs harvested at d 0 and 14 after bleomycin instillation. In situ hybridization was performed to determine the localization of miR-21. Bars: 12.5 µm. (F) Frozen sections were prepared from mouse lungs harvested at d 14 after bleomycin instillation. ISH and immunohistochemistry assays were performed to determine the colocalization of miR-21 and α-SMA (i–iv). An additional slide was processed with H&E staining and an image was obtained from approximately the same regions as shown in i–iv (v). Bars: 20 µm. Results in A–F represent one out of two to three independently performed experiments with similar outcomes. (G) miR-21 levels in histologically normal lungs collected during resection of lung cancer and in lungs from patients with idiopathic pulmonary fibrosis. Experiments were performed with RNA from 8 normal lungs and 8 IPF lungs. Mean ± SEM. *, $P < 0.05$ compared with control normal lungs. (H) In situ hybridization was performed to determine the localization of miR-21 (i) in lung tissue of IPF patients. ISH with scrambled probes (ii). Bars: 20 µm. Experiments were performed twice.

administration (Fig. 2, D and E). The control probes had no effects on bleomycin-induced lung fibrosis (Fig. S2 E). These data indicate that sequestration of miR-21 with antisense probes prevents experimental pulmonary fibrosis. Of note, α-SMA expression was not increased in bleomycin-treated lungs from mice given miR-21 antisense probes, suggesting a role for miR-21 in the induction of myofibroblast differentiation (Fig. 2 E). H&E staining demonstrated dramatic attenuation of bleomycin-induced lung fibrosis in mice pretreated with miR-21 antisense probes; this finding was confirmed by Masson's trichrome staining, which highlights collagen deposition (Fig. 2 F). Likewise, pretreatment with miR-21 antisense probes prevented the accumulation of myofibroblasts in bleomycin-treated lungs, as demonstrated by immunohistochemistry staining with anti α-SMA antibody (Fig. 2 G).

To explore if inhibition of miR-21 has therapeutic potential in the treatment of lung fibrosis, we administered miR-21 antisense probes i.p. once a day from d 5 to 7 after intratracheal instillation of bleomycin, a time when inflammatory responses start to subside and active fibrogenesis occurs (Vittal et al., 2005; Moore and Hogaboam, 2008), and then analyzed the extent of lung fibrosis 14 d after administration of bleomycin. Under these conditions, the majority

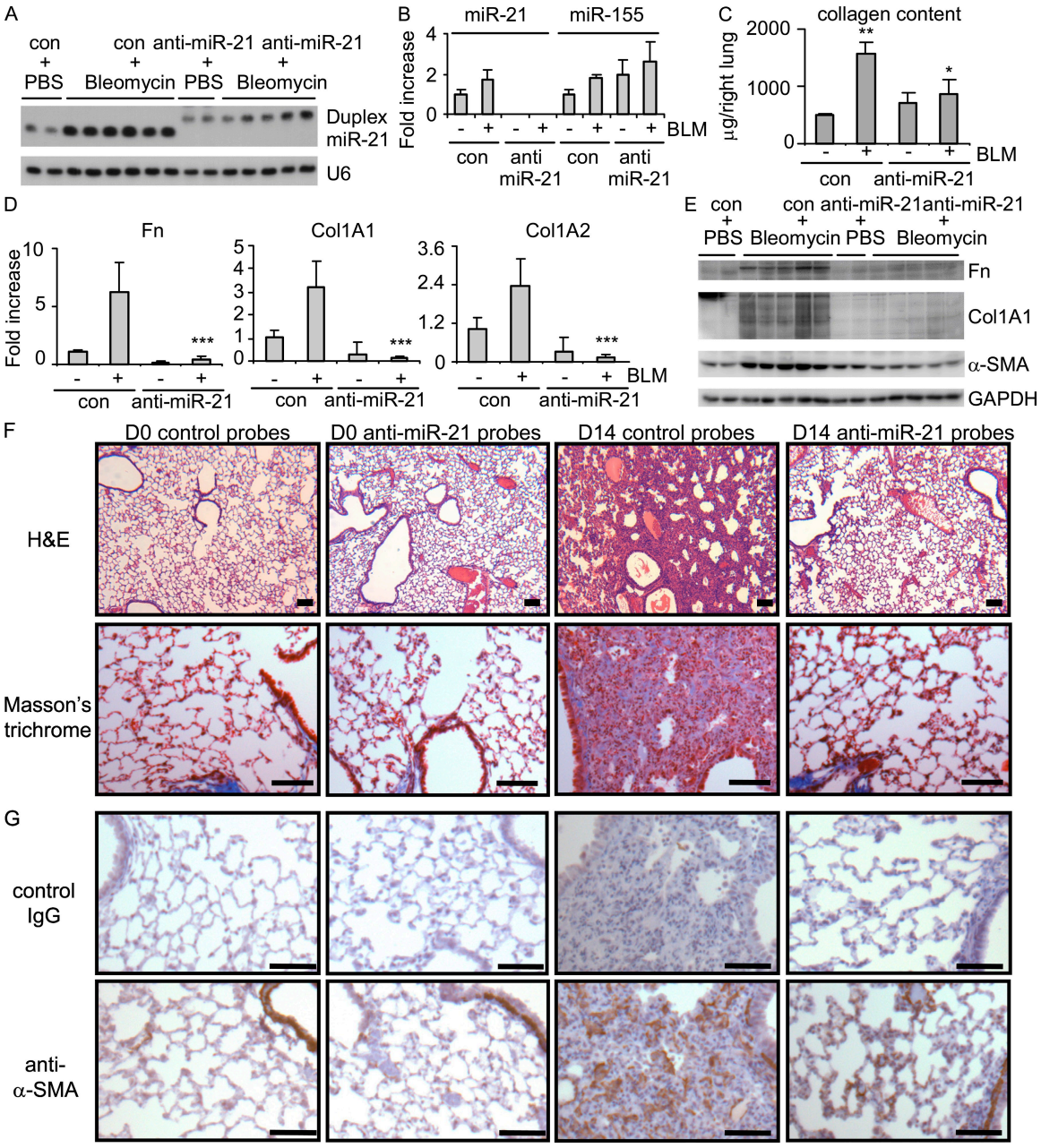

Figure 2. Sequestering miR-21 prevents bleomycin-induced lung fibrosis in mice. (A) Mice (n = 3–6 in each group) received either control probes or miR-21 antisense probes (10 mg/kg body weight in 50 µl PBS) intratracheally on d 4 and 2 before intratracheal instillation of bleomycin (1.5 U/kg in 50 µl PBS) or PBS. At 14 d after bleomycin administration, mice were sacrificed and total RNA from lungs was isolated. Northern blotting was performed to determine miR-21 levels. U6 was the loading control. Representative results are shown. (B) Real-time PCR was performed to determine the levels of miR-21 and miR-155 in two samples from each group described in A. Mean ± SD. (C) Experiments were performed as described in A and collagen content in the right lungs was determined. n = 3–6 mice in each group. Mean ± SEM. **, $P < 0.01$ compared with PBS-treated mice given control probes. *, $P < 0.05$ compared with bleomycin-treated mice given control probes. (D) Real-time PCR was performed to determine mRNA levels of Fn, Col1A1, and Col1A2 in the same samples analyzed in A. n = 3–6 mice in each group. Mean ± SD. ***, $P < 0.001$ compared with bleomycin-treated mice given control probes. (E) Experiments were performed as described in A. Protein levels of Fn, Col1A, α-SMA, and GAPDH in lung homogenates were determined by Western blotting. Results in A–E represent one out of two independently performed experiments. (F) Experiments were performed as described in A. Pulmonary fibrosis, as assessed on d 0 and 14 after bleomycin administration, was determined in mice given control or miR-21 antisense probes. H&E staining and Masson's trichrome blue staining for collagen. Bars: 100 µm. (G) Experiments were performed as described in A. α-SMA expression was determined by immunohistochemistry on d 0 and 14 after bleomycin administration in the lungs of mice given either control probes or miR-21 antisense probes. Mouse IgG was used as a negative control for anti–α-SMA antibodies. Bars: 50 µm. Data presented in F and G are representative of results from two independent experiments with two to three mice in each group.

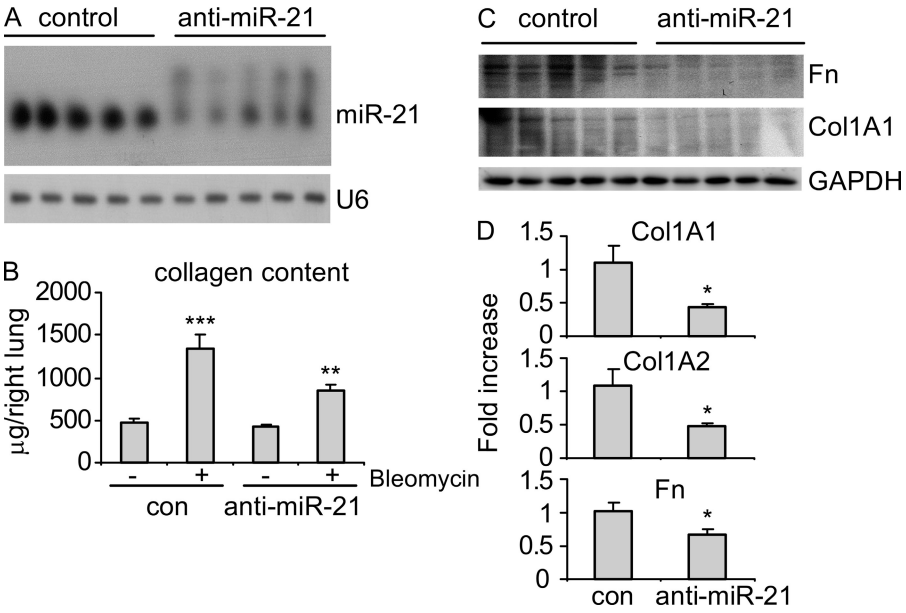

Figure 3. Sequestering miR-21 diminishes the severity of bleomycin-induced lung fibrosis in mice. (A) Mice were given bleomycin intratracheally (1 U/kg in 50 µl PBS). On d 5, 6, and 7 after bleomycin administration, control probes or miR-21 antisense probes (10 mg/kg body weight in 200 µl PBS) were injected i.p. On d 14 after bleomycin instillation, mouse lungs were collected. Northern blotting was performed to determine miR-21 levels using U6 as a loading control. (B) Experiments were performed as described in A. Collagen content was measured in the right lungs. $n = 3–5$ in each group, values are shown as mean ± SEM. ***, $P < 0.001$ compared with mice treated with PBS and control probes. **, $P < 0.01$ compared with mice treated with bleomycin and control probes. (C) Experiments were performed as described in A and mRNA levels of Col1A1, Col1A2, and Fn determined in lungs isolated from the treated mice. (D) Experiments were performed as described in A. Protein levels of Fn, Col1A, and GAPDH in lung homogenates were determined by Western blotting. Experiments were performed twice with similar results.

of mature miR-21 appeared to be sequestered (Fig. 3 A), and miR-21 antisense probes attenuated collagen deposition (Fig. 3 B) as well as Fn and collagen expression at both RNA and protein levels in bleomycin-treated lungs (Fig. 3, C and D). To further define the therapeutic potential of miR-21 sequestration, we administered miR-21 antisense probes intratracheally on d 7 after intratracheal instillation of bleomycin and then determined the extent of fibrosis in the lungs 3 wk after bleomycin injection. As shown in Fig. S2 A, intratracheal instillation of miR-21 antisense probes after bleomycin administration sequestered miR-21 in mouse lungs. Collagen deposition in the lungs was significantly attenuated 3 wk after bleomycin administration in anti-miR-21–treated mice (Fig. S2 B). Administration of miR-21 antisense probes intratracheally on d 14 after intratracheal instillation of bleomycin was still able to attenuate lung fibrosis, although the effects were less significant than those in mice that were treated with anti–miR-21 probes at earlier time points (Fig. S2, C and D).

Pulmonary fibroblasts are primary effectors of lung fibrotic diseases (Hinz et al., 2007). TGF-β1 induces fibroblast differentiation into more fibrogenic myofibroblasts (Hinz et al., 2007). We showed above that enhanced miR-21 expression in bleomycin-treated mice was primarily localized to α-SMA–expressing myofibroblasts. To determine if the mechanisms leading to the anti-fibrotic effects of miR-21 antisense probes in vivo involve potential regulation of fibrogenic activities of pulmonary fibroblasts by miR-21, we studied the role of miR-21 in the activation of pulmonary fibroblasts by TGF-β1. TGF-β1 up-regulated miR-21 expression in a dose- and time-dependent manner in pulmonary fibroblasts (Fig. 4, A and B; Fig. S3 A), suggesting the potential involvement of miR-21 in TGF-β1–related signaling events. Increasing miR-21 levels by transfection of miR-21 precursors enhanced TGF-β1–induced transcription of Fn and α-SMA in pulmonary fibroblasts (Fig. 4 C). Conversely, knocking down miR-21 attenuated TGF-β1–dependent transcription of Fn and α-SMA (Fig. 4 D). Similarly, increasing miR-21 levels enhanced, whereas knocking down miR-21 attenuated, Fn and α-SMA protein levels in pulmonary fibroblasts (Fig. 4, E and F). These data suggest that the anti-fibrotic effects of miR-21 antisense probes may be mediated through regulation of TGF-β1–related signaling events. Consistent with this hypothesis, increasing miR-21 levels enhanced, whereas knocking down miR-21 attenuated, Smad2 phosphorylation in response to TGF-β1 stimulation (Fig. 4, G and H).

Because miR-21 regulates TGF-β1 signaling events under in vitro conditions in pulmonary fibroblasts, we expected that it also might have such actions in vivo. In bleomycin-treated mice, administration of miR-21 antisense probes attenuated Smad2 phosphorylation in the lungs (Fig. 4 I), an event mediated by TGF-β1 activation (Wang et al., 2006). The computational algorithm TargetScan predicted that Smad7, an inhibitory Smad, is a miR-21 target. Consistent with this prediction, up-regulating miR-21 levels decreased, whereas blocking miR-21 increased, Smad7 expression in pulmonary fibroblasts (Fig. 4, J and K). Smad7 expression was also decreased in bleomycin-treated lungs, concomitant with enhanced miR-21 expression under these conditions. Treatment with miR-21 antisense probes prevented the decrease in Smad7 expression in bleomycin-treated lungs (Fig. 4 L). These data suggest that miR-21 targets Smad7 to enhance signaling events downstream of TGF-β1. To determine if miR-21 directly regulates Smad7 expression, the 3′ UTR of the *Smad7* gene was cloned into a luciferase reporter, pMIR-reporter. A 3′ UTR mutant that contains mutations in the

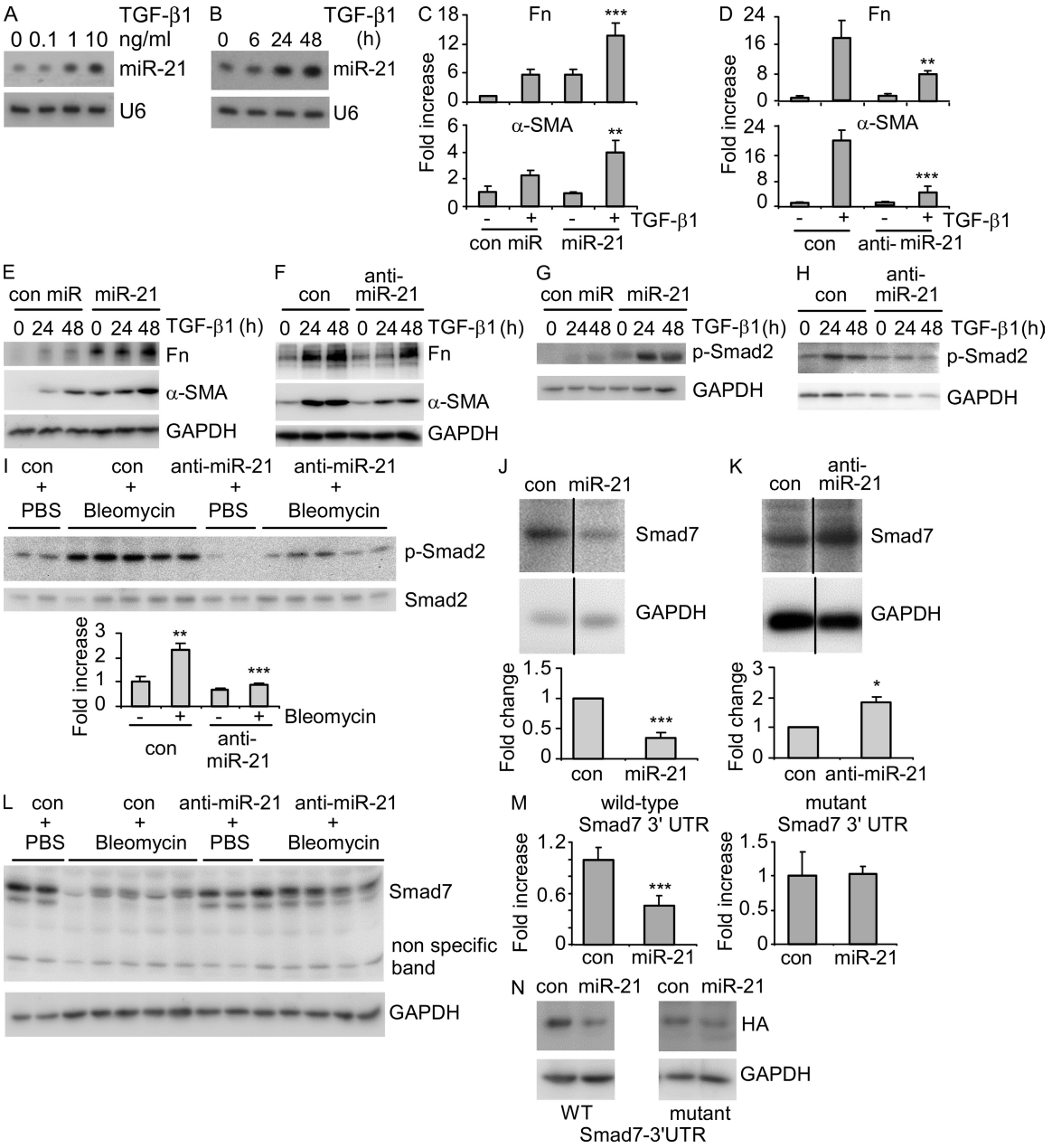

Figure 4. miR-21 is induced by TGF-β1 and regulates the pro-fibrogenic activities of TGF-β1. (A and B) MRC-5 human primary fibroblasts were treated with TGF-β1 at the indicated concentrations for 48 h (A) or 10 ng/ml TGF-β1 for the indicated length of time (B). miR-21 levels were determined by Northern blotting. The small nucleolar RNA, U6, was used as a loading control. The experiments were performed twice with similar results. (C and D) Fibroblasts were transfected with 30 nM control miRNA precursors (C), miR-21 precursors (C), control knockdown probes (D), or miR-21 knockdown probes (D). 2 d after transfection, the fibroblasts were treated with 10 ng/ml TGF-β1 for 48 h. miRNA levels of Fn and α-SMA were determined. Each condition included 3–4 wells. Mean ± SD. **, $P < 0.01$; ***, $P < 0.001$ compared with TGF-β1–treated cells transfected with control probes. Results represent one out of two to three independently performed experiments with similar outcomes. (E–H) Fibroblasts were transfected with control miRNA precursors (E and G), miR-21 precursors (E and G), control knockdown probes (F and H), or miR-21 knockdown probes (F and H), and after 48 h the cells were treated with 2 ng/ml TGF-β1 for an additional 0, 24, or 48 h. Protein levels of Fn, α-SMA, p-Smad2, and GAPDH were determined. Results in E–H represent one out of two to three independently performed experiments with similar outcomes. (I) Protein levels of p-Smad2 and Smad2 in the same samples as shown in Fig. 2 E. Densitometry was performed and fold increase in p-Smad2 expression after normalization to total Smad2 expression is shown. The value for the PBS group with control probes was considered to be 1. **, $P < 0.01$ compared with the PBS group; ***, $P < 0.001$ compared with the bleomycin group treated with control probes. Experiments were performed twice with similar results. (J–K) Fibroblasts were transfected with control miRNA precursors (J), miR-21 precursors (J), control knockdown probes (K), or anti-miR-21 probes (K), and 96 h later the cells were collected and protein levels of Smad7 and GAPDH were determined. The two individual bands separated by the line in J or K were from the same blot. Experiments were performed at least three times. Densitometry analysis was performed and fold increase in Smad7 expression after normalization to GAPDH expression is shown.

predicted miR-21 seeding sequence was also cloned into the pMIR-reporter (Fig. S4 A). Transfection of miR-21 precursors significantly down-regulated luciferase activity for the reporter containing wild-type, but not mutant, *Smad7* 3′ UTR (Fig. 4 M), consistent with direct regulation of Smad7 by miR-21. Furthermore, the Smad7-expressing vector containing wild-type, but not mutant *Smad7* 3′ UTR, was subject to regulation by miR-21 (Fig. 4 N).

In this study, we showed that expression of miR-21 is increased in the lungs of bleomycin-treated mice and in the lungs of patients with IPF. miR-21 expression was enhanced in locations with fibroblast/myofibroblast accumulation and was localized to myofibroblasts. TGF-β1–induced miR-21 expression and miR-21 in turn promoted TGF-β1–induced fibrogenic activation of pulmonary fibroblasts by targeting the inhibitory Smad, Smad7. Thus, miR-21 appears to function in an amplifying circuit to enhance TGF-β1 signaling events and to promote fibrotic lung diseases in which TGF-β plays a contributory role, including IPF.

miRNAs normally have multiple targets (Bushati and Cohen, 2007; Lodish et al., 2008). Though Smad7 was previously shown to negatively regulate lung fibrosis (Nakao et al., 1999; Shukla et al., 2009), inhibition of Smad7 may not be the sole mechanism by which miR-21 exerts profibrogenic effects. For example, Spry1, a negative regulator of Erk activation, was previously shown to be a miR-21 target (Thum et al., 2008). Erk activation has been demonstrated to promote the fibrogenic activities of TGF-β1 (Ding et al., 2008). In our experiments, Spry1 was decreased in bleomycin-treated lungs, whereas Erk phosphorylation was increased (Fig. S4 B). The decrease in Spry1 expression and increase in Erk phosphorylation was prevented in the lungs of mice treated with miR-21 antisense probes (Fig. S4 B). In experimental models of myocardial infarction, phosphatase and tensin homologue (PTEN) was down-regulated by miR-21 in cardiofibroblasts from the infracted areas (Roy et al., 2009). Furthermore, PTEN has been shown to negatively regulate experimental lung fibrosis (White et al., 2006). Such studies suggest that PTEN could also be involved in the profibrotic effects of miR-21. Thus, miR-21 occupies an important role in integrating functionally connected pathways involved in pulmonary fibrotic disease through its ability to regulate multiple important signaling events involved in fibrogenesis. Targeting miR-21 in IPF may represent a better therapeutic strategy than approaches aimed at a single pathway. Our data highlight the ability of miRNAs to fine tune various cellular and developmental events, rather than abolishing the expression of a single protein (Bushati and Cohen, 2007; Lodish et al., 2008).

Although TGF-β1 is an important mediator of fibrotic diseases, it may not be the only factor causing miR-21 up-regulation during fibrosis, as indicated by our data that miR-21 was still up-regulated in the lungs of mice expressing dominant-negative TGF-β1RII after intratracheal administration of bleomycin, although to a lesser extent than in wild-type mice (Fig. S1 C). Other pro-fibrotic growth factors, such as EGF signaling, have been shown to regulate miR-21 expression in cancer cells (Seike et al., 2009). We found that bFGF, another important profibrotic growth factor involved in the pathogenesis of IPF (Inoue et al., 2002), enhances miR-21 expression in human primary fibroblasts (Fig. S3 B). Thus, dysregulation of miR-21 could arise from aberrations in multiple critical signaling events involved in pulmonary fibrosis.

Our studies provide proof of concept and suggest a novel approach using miRNA therapeutics, specifically directed to miR-21, in treating clinically important fibrotic diseases such as IPF, for which cures have long been elusive.

MATERIALS AND METHODS

Experimental pulmonary fibrosis model. C57BL/6 mice were purchased from NCI-Frederick. Transgenic mice that inducibly express a dominant-negative form of TGF-β1RII were a gift from Drs. Rosa Serra and Namasivayam Ambalavanan (University of Alabama at Birmingham, Birmingham, AL). To induce the expression of dominant-negative TGF-β1RII, mice were given water containing 10 mM $ZnSO_4$ for 2 wk before intratracheal administration of bleomycin and kept on $ZnSO_4$-containing water for the entire period of the experiments. As controls, wild-type mice were provided with the same $ZnSO_4$-containing water. For bleomycin instillation, 8-wk-old mice were anesthetized with isoflurane. After the tongues of the anesthetized mice were gently pulled forward with forceps, bleomycin (from EMD; 1–1.5 U/kg body weight in 50 µl PBS) was delivered into the oropharyngeal cavity. The tongue was kept extended until all of the liquid was inhaled into the lungs. The mice were sacrificed at the indicated time points. The animal protocol was approved by the UAB Institutional Animal Care and Use Committee (IACUC).

Reagents. Human recombinant TGF-β1 was purchased from PeproTech. LNA-modified control knockdown and miR-21 knockdown probes for in vivo applications were synthesized by Exiqon.

Cell culture. Human primary pulmonary cell lines, MRC-5 and IMR-90, as well as HEK-293 cells, were purchased from American Type Culture Collection (Manassas, VA). Cells were cultured at 37°C with 5% CO_2 in DME containing 10% FBS.

Human lung tissue. 8 IPF lung tissue samples were obtained from surgical remnants of biopsies or lungs explanted from patients with IPF that underwent pulmonary transplant and 8 controls were obtained through the University of Pittsburgh Health Sciences Tissue Bank from samples resected from patients with lung cancer. The protocol was approved by the Institutional Review Board (IRB) of the University of Pittsburgh.

***, $P < 0.001$ compared with the group treated with control precursors; *, $P < 0.05$ compared with the group with control anti-miR probes. (L) Protein levels of Smad7 and GAPDH in the same samples shown in Fig. 2 E. Experiments were performed twice with similar results. (M) Luciferase reporters containing wild-type or mutant 3′ UTR of mouse *smad7* gene were cotransfected with control miRNA or miR-21 precursors into HEK-293 cells. 2 d after transfection, dual luciferase activity was measured. ***, $P < 0.001$ compared with cells transfected with con mimics. (N) HA-smad7–expressing vector that contains wild-type or mutant 3′ UTR of the mouse *smad7* gene was cotransfected with control vectors or vectors expressing miR-21 into HEK-293 cells. 2 d after transfection, HA-smad7 levels were determined. Experiments in M and N were performed two to three times with similar results.

miRNA array. Total RNAs were isolated from mouse lungs harvested at d 0, 7, and 14 after bleomycin instillation (three mice per group) with the smiRNAeasy Mini kit (QIAGEN). The miRNA array was performed by Exiqon using miRCURY LNA microRNA Array (Exiqon). Array Express accession no. E-MEXP-2749.

Northern blotting. The assay was performed as described previously (Liu et al., 2009). In brief, total RNA (10 μg) was resolved on a 12% denatured polyacrylamide gel containing 8M urea. The RNA was then transferred to a Hybond nylon membrane (GE Life Sciences). After UV cross-linking, the membrane was incubated in prehybridization buffer (50% formamide [USB], 0.5% SDS, 5xSSC [USB], 5×Denhardt's solution [USB], and 20 μg/ml sheared, denatured, salmon sperm DNA [Invitrogen]) at 55°C for 30 min and then hybridized with specific γ[P^{32}]-labeled human LNA miR-21 probes (Exiqon) at 55°C for 24 h. The membrane was washed for 10 min three times with buffer (0.5% SDS, 2xSSC) and exposed to film. After hybridization with miR-21 probes, the membrane was stripped and reblotted with specific γ[P^{32}]-labeled mouse U6 probes (Exiqon) as loading controls.

Real-time PCR. The assay was performed as described previously (Liu et al., 2009). Taqman probes for hsa-miR-21, hsa-miR-155, and mouse Sno135 were purchased from Applied Biosystems. The expression of α-SMA, fibronectin, Col1A1, Col1A2, and TGF-β1 was determined using the SYBR Green Master Mix kit (Roche). GAPDH or HPRT was used as an internal control. The sequences of the primers: mouse HPRT: sense, 5′-GGGACATAAAAGTTATTGGTGGAGATG-3′; antisense, 5′-CAACAAACTTGTCTGGAATTTCAA-3′. Human fibronectin: sense, 5′-GTGTTGGGAATGGTCGTGGGGAATG-3′; antisense, 5′-CCAATGCCACGGCCATAGCAGTAGC-3′. Mouse fibronectin: sense, 5′-TCTGGGAAATGGAAAAGGGGAATGG-3′; antisense, 5′-CACTGAAGCAGGTTTCCTCGGTTGT-3′. Human α-SMA: sense, 5′-CATCACCAACTGGGACGACATGGAA-3′; antisense, 5′-GCATAGCCCTCATAGATGGGGACATTG-3′. Mouse α-SMA: sense, 5′-GACGCTGAAGTATCCGATAGAACACG-3′; antisense 5′-CACCATCTCCAGAGTCCAGCACAAT-3′. Mouse TGF-β1: sense, 5′-AGCGGACTACTATGCTAAAGAGGTCACCC-3′; antisense, 5′-CCAAGGTAACGCCAGGAATTGTTGCTATA-3′. Mouse Col1A1: sense, 5′-GGAGGGCGAGTGCTGTGCTTT-3′; antisense, 5′-GGGACCAGGAGGACCAGGAAGT-3′. Mouse Col1A2: sense, 5′-TGGTCTTACTGGGAACTTTGCTGC-3′; antisense, 5′-ACCCTGTGGTCCAACGACTCCTCTC-3′. Mouse GAPDH: sense, 5′-CGACTTCAACAGCAACTCCCACTCTTCC-3′; antisense, 5′-TGGGTGGTCCAGGGTTTCTTACTCCTT-3′. Human GAPDH: sense, 5′-GCTGGCGCTGAGTACGTCGTGGAGT-3′; antisense, 5′-CACAGTCTTCTGGGTGGCAGTGATGG-3′.

In situ hybridization (ISH). The assay was performed as described previously (Obernosterer et al., 2007). In brief, mice were sacrificed and the lungs inflated with intratracheal injection of 1 ml OCT (Thermo Fisher Scientific). The lungs were then embedded with OCT, and 10-μm-thick frozen sections prepared. The sections were dried at room temperature for 30 min, followed by fixation in 4% paraformaldehyde (Thermo Fisher Scientific) for 30 min. The sections were treated in acetylation solution for 10 min and then in PBS containing 10 μg/ml proteinase K (Sigma-Aldrich) for 5 min. Sections were then blocked with hybridization solution for 4 h at room temperature and incubated with digoxigenin (Dig)-conjugated miR-21 probes (Exiqon) or Dig-conjugated control probes with scrambled sequence (Exiqon) overnight. The sections were washed with 0.2× SSC followed by incubation with HRP-conjugated anti-Dig antibody (Roche) overnight at 4°C. After washing three times with buffer B1, the sections were developed with NBT/BCIP (Roche) for 24 h, with light blue cytoplasmic staining being positive. To determine the colocalization of miR-21 and α-SMA, FITC-conjugated miR-21 probes (Exiqon) in combination with Cy3-conjugated anti–α-SMA antibody (Sigma-Aldrich) were used in the hybridization assays. The sections were examined by confocal microscopy. miR-21 was shown as green fluorescence and α-SMA as red fluorescence.

Immunohistochemistry. Mouse lungs were inflated with 10% formalin solution and embedded in paraffin. 10-μm-thick sections were prepared, deparaffinized with xylene, and then rehydrated in water through graded ethanol. Antigen retrieval was performed in a pressure cooker in Tris-EDTA solution, pH 9.0, for 5 min. After incubation in TBST buffer for 10 min and 3% H_2O_2 for 10 min, the sections were washed with TBST and blocked with avidin/biotin blocker and affinity-purified goat anti–mouse IgG (H+L). The sections were then incubated with mouse anti–α-SMA (Sigma-Aldrich) overnight at 4°C, secondary antibody for 45 min, avidin-HRP for 45 min, and DAB chromagen, sequentially. Finally, the sections were counterstained with hematoxylin.

Collagen content determination. The right lungs from mice were collected and homogenized in 5 ml 0.5 M acetic acid in PBS containing 0.6% pepsin. The extracts were rotated at 4°C overnight and cleared by centrifugation at 13,200 rpm for 15 min. Collagen content was measured using the Sircol Collagen Assay kit (Biocolor Ltd.) according to the manufacturer's instructions. Collagen content is presented as μg acid-soluble collagen/right lung.

Western blotting. Western blotting was performed as described previously (Liu et al., 2008). Mouse anti-Fn antibody, goat anti-Col1A1 antibodies, rabbit anti-GAPDH antibodies, and rabbit anti-Spry1 antibodies were from Santa Cruz Biotechnology, Inc. Mouse anti–α-SMA was from Sigma-Aldrich. Rabbit anti–p-Smad2, Smad-2, P-Erk, and Erk were from Cell Signaling Technology. Rabbit anti-Smad7 antibodies were from Thermo Fisher Scientific.

Luciferase reporter assay. The full-length 3′ UTR of mouse *Smad7* gene was amplified by PCR using mouse genomic DNA as a template. The primers were: sense 5′-ACTAGTACCGTTCAAACTACTTGCTGCTAACC-3′ and antisense 5′-AAGCTTTGCTAAATTTCCAATGAGAATGCTTC-3′. The PCR fragment was cloned downstream of the luciferase gene between the SpeI and HindIII sites in pMIR-Report (Applied Biosystems). To generate Smad7 3′ UTR mutants containing mutations in the conserved miR-21 binding site, site-directed mutagenesis was performed using the wild-type 3′ UTR as the template. In the 3′ UTR mutant, the nucleotide sequence complementary to nt 2–5 of miR-21 was mutated to the same sequence as that in miR-21 (from AGCT to TCGA). 0.5 μg of the luciferase reporters containing the wild-type or mutant 3′ UTR were cotransfected with control miRNA precursors or miR-21 precursors into HEK-293 cells. As an internal control, renilla luciferase reporters were also included. 2 d after transfection, the cells were collected and dual luciferase activities were measured according to the manufacturer's instructions.

Masson's trichrome assay. The assay was performed by the UAB Tissue Histology Core facility as described previously (Hecker et al., 2009).

H&E staining. The assay was performed by the UAB Tissue Histology Core facility as described previously (Hecker et al., 2009).

Statistical analysis. One-way ANOVA followed by the Holm-Sidak or Tukey-Kramer test was performed for multiple group comparisons. The Student's *t* test was used for comparison between two groups. $P < 0.05$ was considered significant.

Online supplemental material. Fig. S1 shows enhanced expression of miR-21 in the lungs of mice with experimental lung fibrosis. Fig. S2 shows that sequestering miR-21 attenuates experimental lung fibrosis in mice. Fig. S3 demonstrates that miR-21 is induced by TGF-β1 and bFGF in human primary fibroblasts. Fig. S4 shows that miR-21 regulates Smad7 and Spry1. Online supplemental material is available at http://www.jem.org/cgi/content/full/jem.20100035/DC1.

G. Liu conceived of, designed, conducted, and supervised the experiments. A. Friggeri and Y. Yang contributed to mouse studies. J. Milosevic, Q. Ding,

V.J. Thannickal, and N. Kaminski contributed to the data on human samples. E. Abraham designed and supervised the study. G. Liu and E. Abraham wrote the manuscript.

The authors thank Drs. Rosa Serra and Namasivayam Ambalavanan at the University of Alabama at Birmingham for supplying transgenic mice expressing dominant-negative TGF-β1RII. The authors also thank Drs. Dezhi Wang and Lingling Guo of UAB for technical assistance in mouse studies.

This work was supported by National Institutes of Health grants R21HL097218 (to G. Liu), R01HL076206 (to E. Abraham), R01GM87748 (to E. Abraham), R01LM009657 (to. N. Kaminski), and R01HL095397 (to. N. Kaminski). N. Kaminski is the Simmons Endowed Chair for Pulmonary Research.

The authors have no conflicting financial interests.

Submitted: 5 January 2010
Accepted: 23 June 2010

REFERENCES

Ambalavanan, N., T. Nicola, J. Hagood, A. Bulger, R. Serra, J. Murphy-Ullrich, S. Oparil, and Y.F. Chen. 2008. Transforming growth factor-beta signaling mediates hypoxia-induced pulmonary arterial remodeling and inhibition of alveolar development in newborn mouse lung. *Am. J. Physiol. Lung Cell. Mol. Physiol.* 295:L86–L95. doi:10.1152/ajplung.00534.2007

Bushati, N., and S.M. Cohen. 2007. microRNA functions. *Annu. Rev. Cell Dev. Biol.* 23:175–205. doi:10.1146/annurev.cellbio.23.090506.123406

Croce, C.M. 2009. Causes and consequences of microRNA dysregulation in cancer. *Nat. Rev. Genet.* 10:704–714. doi:10.1038/nrg2634

Cutroneo, K.R., S.L. White, S.H. Phan, and H.P. Ehrlich. 2007. Therapies for bleomycin induced lung fibrosis through regulation of TGF-beta1 induced collagen gene expression. *J. Cell. Physiol.* 211:585–589. doi:10.1002/jcp.20972

Davis, B.N., A.C. Hilyard, G. Lagna, and A. Hata. 2008. SMAD proteins control DROSHA-mediated microRNA maturation. *Nature.* 454:56–61. doi:10.1038/nature07086

Ding, Q., C.L. Gladson, H. Wu, H. Hayasaka, and M.A. Olman. 2008. Focal adhesion kinase (FAK)-related non-kinase inhibits myofibroblast differentiation through differential MAPK activation in a FAK-dependent manner. *J. Biol. Chem.* 283:26839–26849. doi:10.1074/jbc.M803645200

Elmén, J., M. Lindow, S. Schütz, M. Lawrence, A. Petri, S. Obad, M. Lindholm, M. Hedtjärn, H.F. Hansen, U. Berger, et al. 2008. LNA-mediated microRNA silencing in non-human primates. *Nature.* 452:896–899. doi:10.1038/nature06783

Hardie, W.D., S.W. Glasser, and J.S. Hagood. 2009. Emerging concepts in the pathogenesis of lung fibrosis. *Am. J. Pathol.* 175:3–16. doi:10.2353/ajpath.2009.081170

Hecker, L., R. Vittal, T. Jones, R. Jagirdar, T.R. Luckhardt, J.C. Horowitz, S. Pennathur, F.J. Martinez, and V.J. Thannickal. 2009. NADPH oxidase-4 mediates myofibroblast activation and fibrogenic responses to lung injury. *Nat. Med.* 15:1077–1081. doi:10.1038/nm.2005

Hinz, B., S.H. Phan, V.J. Thannickal, A. Galli, M.L. Bochaton-Piallat, and G. Gabbiani. 2007. The myofibroblast: one function, multiple origins. *Am. J. Pathol.* 170:1807–1816. doi:10.2353/ajpath.2007.070112

Inoue, Y., T.E. King Jr., E. Barker, E. Daniloff, and L.S. Newman. 2002. Basic fibroblast growth factor and its receptors in idiopathic pulmonary fibrosis and lymphangioleiomyomatosis. *Am. J. Respir. Crit. Care Med.* 166:765–773. doi:10.1164/rccm.2010014

Latronico, M.V., and G. Condorelli. 2009. MicroRNAs and cardiac pathology. *Nat Rev Cardiol.* 6:419–429. doi:10.1038/nrcardio.2009.56

Lee, C.G., S. Cho, R.J. Homer, and J.A. Elias. 2006. Genetic control of transforming growth factor-beta1-induced emphysema and fibrosis in the murine lung. *Proc. Am. Thorac. Soc.* 3:476–477. doi:10.1513/pats.200603-040MS

Liu, G., Y.J. Park, and E. Abraham. 2008. Interleukin-1 receptor-associated kinase (IRAK)-1-mediated NF-kappaB activation requires cytosolic and nuclear activity. *FASEB J.* 22:2285–2296. doi:10.1096/fj.07-101816

Liu, G., A. Friggeri, Y. Yang, Y.J. Park, Y. Tsuruta, and E. Abraham. 2009. miR-147, a microRNA that is induced upon Toll-like receptor stimulation, regulates murine macrophage inflammatory responses. *Proc. Natl. Acad. Sci. USA.* 106:15819–15824. doi:10.1073/pnas.0901216106

Lodish, H.F., B. Zhou, G. Liu, and C.Z. Chen. 2008. Micromanagement of the immune system by microRNAs. *Nat. Rev. Immunol.* 8:120–130. doi:10.1038/nri2252

Moore, B.B., and C.M. Hogaboam. 2008. Murine models of pulmonary fibrosis. *Am. J. Physiol. Lung Cell. Mol. Physiol.* 294:L152–L160. doi:10.1152/ajplung.00313.2007

Nakao, A., M. Fujii, R. Matsumura, K. Kumano, Y. Saito, K. Miyazono, and I. Iwamoto. 1999. Transient gene transfer and expression of Smad7 prevents bleomycin-induced lung fibrosis in mice. *J. Clin. Invest.* 104:5–11. doi:10.1172/JCI6094

Obernosterer, G., J. Martinez, and M. Alenius. 2007. Locked nucleic acid-based in situ detection of microRNAs in mouse tissue sections. *Nat. Protoc.* 2:1508–1514. doi:10.1038/nprot.2007.153

Pandey, A.K., P. Agarwal, K. Kaur, and M. Datta. 2009. MicroRNAs in diabetes: tiny players in big disease. *Cell. Physiol. Biochem.* 23:221–232. doi:10.1159/000218169

Pandit, K.V., D. Corcoran, H. Yousef, M. Yarlagadda, A. Tzouvelekis, K.F. Gibson, K. Konishi, S.A. Yousem, M. Singh, D. Handley, et al. 2010. Inhibition and role of let-7d in idiopathic pulmonary fibrosis. *Am. J. Respir. Crit. Care Med.* In press. doi: 10.1164/rccm.200911-1698OC

Roy, S., S. Khanna, S.R. Hussain, S. Biswas, A. Azad, C. Rink, S. Gnyawali, S. Shilo, G.J. Nuovo, and C.K. Sen. 2009. MicroRNA expression in response to murine myocardial infarction: miR-21 regulates fibroblast metalloprotease-2 via phosphatase and tensin homologue. *Cardiovasc. Res.* 82:21–29. doi:10.1093/cvr/cvp015

Seike, M., A. Goto, T. Okano, E.D. Bowman, A.J. Schetter, I. Horikawa, E.A. Mathe, J. Jen, P. Yang, H. Sugimura, et al. 2009. MiR-21 is an EGFR-regulated anti-apoptotic factor in lung cancer in never-smokers. *Proc. Natl. Acad. Sci. USA.* 106:12085–12090. doi:10.1073/pnas.0905234106

Shukla, M.N., J.L. Rose, R. Ray, K.L. Lathrop, A. Ray, and P. Ray. 2009. Hepatocyte growth factor inhibits epithelial to myofibroblast transition in lung cells via Smad7. *Am. J. Respir. Cell Mol. Biol.* 40:643–653. doi:10.1165/rcmb.2008-0217OC

Stefani, G., and F.J. Slack. 2008. Small non-coding RNAs in animal development. *Nat. Rev. Mol. Cell Biol.* 9:219–230. doi:10.1038/nrm2347

Thannickal, V.J., G.B. Toews, E.S. White, J.P. Lynch III, and F.J. Martinez. 2004. Mechanisms of pulmonary fibrosis. *Annu. Rev. Med.* 55:395–417. doi:10.1146/annurev.med.55.091902.103810

Thum, T., C. Gross, J. Fiedler, T. Fischer, S. Kissler, M. Bussen, P. Galuppo, S. Just, W. Rottbauer, S. Frantz, et al. 2008. MicroRNA-21 contributes to myocardial disease by stimulating MAP kinase signalling in fibroblasts. *Nature.* 456:980–984. doi:10.1038/nature07511

Tomasek, J.J., G. Gabbiani, B. Hinz, C. Chaponnier, and R.A. Brown. 2002. Myofibroblasts and mechano-regulation of connective tissue remodelling. *Nat. Rev. Mol. Cell Biol.* 3:349–363. doi:10.1038/nrm809

Vittal, R., J.C. Horowitz, B.B. Moore, H. Zhang, F.J. Martinez, G.B. Toews, T.J. Standiford, and V.J. Thannickal. 2005. Modulation of prosurvival signaling in fibroblasts by a protein kinase inhibitor protects against fibrotic tissue injury. *Am. J. Pathol.* 166:367–375.

Wang, X.M., Y. Zhang, H.P. Kim, Z. Zhou, C.A. Feghali-Bostwick, F. Liu, E. Ifedigbo, X. Xu, T.D. Oury, N. Kaminski, and A.M. Choi. 2006. Caveolin-1: a critical regulator of lung fibrosis in idiopathic pulmonary fibrosis. *J. Exp. Med.* 203:2895–2906. doi:10.1084/jem.20061536

White, E.S., R.G. Atrasz, B. Hu, S.H. Phan, V. Stambolic, T.W. Mak, C.M. Hogaboam, K.R. Flaherty, F.J. Martinez, C.D. Kontos, and G.B. Toews. 2006. Negative regulation of myofibroblast differentiation by PTEN (Phosphatase and Tensin Homolog Deleted on chromosome 10). *Am. J. Respir. Crit. Care Med.* 173:112–121. doi:10.1164/rccm.200507-1058OC

Wynn, T.A. 2007. Common and unique mechanisms regulate fibrosis in various fibroproliferative diseases. *J. Clin. Invest.* 117:524–529. doi:10.1172/JCI31487

Zhang, K., K.C. Flanders, and S.H. Phan. 1995. Cellular localization of transforming growth factor-beta expression in bleomycin-induced pulmonary fibrosis. *Am. J. Pathol.* 147:352–361.